contrast, the self-cleaning water/solid interfaces achieved by superhydrophilic polyelectrolyte brush surfaces are proposed here.

CONCLUSIONS

Contact angle measurements of water, diiodomethane, hexadecane, and air bubbles were performed to investigate the surface wettabilities of various polymer brushes with hydrophobic perfluoroalkyl and hydrophilic hydroxy groups, amino groups, negatively and positively charged functional groups, and zwitterionic-type electrolyte groups. The fluoropolymer brush had a high water contact angle of up to 121° and a small hysteresis expressed by $\theta_A - \theta_R$, whereas noninoic hydrophilic polymer brushes such as PDHMA, PVA, and POEGMA had relatively small water contact angles and large hystereses. The surface rearrangement of polar functional groups of the polymer brushes might occur as a result of contact with a water droplet in a dry atmosphere. The polyelectrolyte brushes had extremely low water contact angles below 3° and excellent wetting properties with water and hexadecane. The surface free energies of the polyelectrolyte brushes were evaluated to be 70−73 mN/m by Owens' method. Additional theoretical and experimental work is necessary to determine the surface free energy of the polyelectrolyte brushes.

The polyelectrolyte brush surfaces, including PMANa, PSPMK, PMAPS, and PMPC, in aqueous media repelled both air bubbles and hexadecane droplets because of the strong affinity of polyelectrolytes for water. Even when the silicone oil spread on the polyelectrolyte brush surfaces in air, the oil quickly beaded up and detached from the brush surfaces once they were immersed in water. The oil detachment behavior observed on the polyelectrolyte brush in water was explained by the low adhesion force between the hydrate brush and oil, which contributed to excellent antifouling and self-cleaning properties without any surfactants. Thus, one novel strategy for designing a superoleophobic water/solid interface relies on a superhydrophilic surface consisting of ionic polymers, which contrasts with the conventional method using superhydrophobic surfaces. We assume that the fundamental water wettability of various polymer brushes demonstrated in this article is important to the design of surface properties such as friction and adhesion and antifouling properties.

ASSOCIATED CONTENT

Supporting Information

Surface free energy components of the PMMA, PFA-C_8, PMANa, PMTAC, PSPMK, PMAPS, and PMPC brush surfaces and the polyelectrolyte brushes calculated by the vOCG protocol. Videos of the oil detachment behaviors and bouncing air bubble on a polyelectrolyte brush in water. This material is available free of charge via the Internet at http://pubs.acs.org.

AUTHOR INFORMATION

Corresponding Author

*Motoyasu Kobayashi: Phone, +81-92-802-2543; Fax, +81-92-802-2544; E-mail, motokoba@cstf.kyushu-u.ac.jp. *Atsushi Takahara: Phone, +81-92-802-2517; Fax, +81-92-802-2518; E-mail, takahara@cstf.kyushu-u.ac.jp.

Notes

The authors declare no competing financial interest.

ACKNOWLEDGMENTS

We acknowledge Daikin Industries Ltd. for supplying the FA-C_8 monomer.

REFERENCES

(1) Klein, J. Shear, friction, and lubrication forces between polymer-bearing surfaces. *Annu. Rev. Mater. Sci.* **1996**, *26*, 581−612.
(2) Xu, F. J.; Neoh, K. G.; Kang, E. T. Bioactive surfaces and biomaterials via atom transfer radical polymerization. *Prog. Polym. Sci.* **2009**, *34*, 719−761.
(3) Tsuruta, T. Contemporary topics in polymeric materials for biomedical applications. *Adv. Polym. Sci.* **1996**, *126*, 1−51.
(4) Lapčík, L., Jr.; Lapčík, L.; De Dmedt, S.; Demeester, J.; Chabrecek, P. Hyaluronan: preparation, structure, properties, applications. *Chem. Rev.* **1998**, *98*, 2663−2684.
(5) Radaeva, F.; Kostina, G. A.; Zmievskii, A. V. Hyaluronic acid: biological role, structure, synthesis, isolation, purification, and applications. *Appl. Biochem. Microbiol.* **1997**, *33*, 111−115.
(6) Rühe, J. Polymer Brushes: On the Way to Tailor-Made Surfaces. In *Polymer Brushes*; Advincula, R. C., Brittain, W. J.; Caster, K. C., Rühe, J., Eds.; Wiley-VCH: Weinheim, Germany, 2004; pp 1−31.
(7) Chen, Y.; Deng, Q.; Xiao, J.; Nie, H.; Wu, L.; Zhou, W.; Huang, B. Controlled grafting from poly(vinylidene fluoride) microfiltration membranes via reverse atom transfer radical polymerization and antifouling properties. *Polymer* **2007**, *48*, 7604−7613.
(8) Chang, Y.; Liao, S.-C.; Higuchi, A.; Ruaan, R.-C.; Chu, C.-W.; Chen, W.-Y. A highly stable nonbiofouling surface with well-packed grafted zwitterionic polysulfobetaine for plasma protein repulsion. *Langmuir* **2008**, *24*, 5453−5458.
(9) Yang, Y.-F.; Li, Y.; Li, Q.-L.; Wan, L.-S.; Xu, Z.-K. Surface hydrophilization of microporous polypropylene membrane by grafting zwitterionic polymer for anti-biofouling. *J. Membr. Sci.* **2010**, *362*, 255−264.
(10) Muller, P.; Sudre, G.; Théodoly, O. Wetting transition on hydrophobic surfaces covered by polyelectrolyte brushes. *Langmuir* **2008**, *24*, 9541−9450.
(11) Spruijt, E.; Choi, E.-Y.; Huck, W. T. S. Reversible electrochemical switching of polyelectrolyte brush surface energy using electroactive counterions. *Langmuir* **2008**, *24*, 11253−11260.
(12) Ishihara, K.; Ueda, T.; Nakabayashi, N. Preparation of phospholipid polymers and their properties as polymer hydrogel membranes. *Polym. J.* **1990**, *22*, 355−360.
(13) Kobayashi, M.; Terayama, Y.; Hosaka, N.; Kaido, M.; Suzuki, A.; Yamada, N.; Torikai, N.; Ishihara, K.; Takahara, A. Friction behavior of high-density poly(2-methacryloyloxyethyl phosphorylcholine) brush in aqueous media. *Soft Matter* **2007**, *3*, 740−746.
(14) Kobayashi, M.; Takahara, A. Tribological properties of hydrophilic polymer brushes under wet conditions. *Chem. Rec.* **2010**, *10*, 208−216.
(15) Nosonovsky, M.; Bhushan, B. Superhydrophobic surfaces and emerging applications: non-adhesion, energy, green engineering. *Curr. Opin. Colloid Interface Sci.* **2009**, *14*, 270−280.
(16) Koch, K.; Bhushan, B.; Barthlott, W. Multifunctional surface structures of plants: an inspiration for biomimetics. *Prog. Mater. Sci.* **2009**, *54*, 137−178.
(17) Marmur, A. Underwater superhydrophobicity: theoretical feasibility. *Langmuir* **2006**, *22*, 1400−1402.
(18) Lord, M. S.; Stenzel, M. H.; Simmons, A.; Milthorpe, B. K. The effect of charged groups on protein interactions with poly(HEMA) hydrogels. *Biomaterials* **2006**, *27*, 567−575.
(19) Genzer, J.; Efimenko, K. Recent developments in superhydrophobic surfaces and their relevance to marine fouling: a review. *Biofouling* **2006**, *22*, 339−360.
(20) Liu, M.; Wang, S.; Wei, Z.; Song, Y.; Jiang, L. Bioinspired design of a superoleophobic and low adhesive water/solid interface. *Adv. Mater.* **2009**, *21*, 665−669.
(21) Matsumoto, H.; Shinkai, S.; Kineshima, K.; Baba, T.; Ohonuki, T.; Kurauchi, H. JP Patent, P2004-99912A.

(22) Owens, D. K.; Wendt, R. C. Estimation of the surface free energy of polymers. *J. Appl. Polym. Sci.* **1969**, *13*, 1741−1747.
(23) Fowkes, F. M. Additivity of intermolecular forces at interfaces. I. Determination of the contribution to surface and interfacial tensions of dispersion forces in various liquid. *J. Phys. Chem.* **1963**, *67*, 2538−2541.
(24) Fowkes, F. M. Quantitative characterization of the acid-base properties of solvents, polymers, and inorganic surfaces. *J. Adhes. Sci. Technol.* **1990**, *4*, 669−691.
(25) van Oss, C. J.; Chaudhury, M. K.; Good, R. J. Interfacial Lifshitz−van der Waals and polar interactions in macroscopic systems. *Chem. Rev.* **1988**, *88*, 927−941.
(26) Della Volpe, C.; Maniglio, D.; Brugnara, M.; Siboni, S.; Morra, M. The solid surface free energy calculation I. In defense of the multicomponent approach. *J. Colloid Interface Sci.* **2004**, *271*, 434−453.
(27) Chibowski, E.; Perea-Carpio, R. Problems of contact angle and solid surface free energy determination. *Adv. Colloid Interface Sci.* **2002**, *98*, 245−264.
(28) Ozcan, C.; Hasirci, N. Evaluation of surface free energy for PMMA films. *J. Appl. Polym. Sci.* **2008**, *108*, 438−446.
(29) Lewis, L. N.; Stein, J.; Smith, K. A.; Messmer, R. P.; Legrand, D. G.; Scott, R. A. In *Progress in Organosilicon Chemistry*; Marciniec, B., Chhojnowski, J., Eds.; Gordon and Breach Publishers: Langhorne, PA, 1993; pp 263−285.
(30) Tada, H.; Nagatama, H. Chemical vapor surface modification of porous glass with fluoroalkyl-functional silanes. 1. Characterization of the molecular layer. *Langmuir* **1994**, *10*, 1472−1476.
(31) Takahara, A.; Hara, Y.; Kojio, K.; Kajiyama, T. Plasma protein adsorption behavior onto the surface of phase-separated organosilane monolayers on the basis of scanning force microscopy. *Colloids Surf., B* **2002**, *23*, 141−152.
(32) Husseman, M.; Malmstrom, E. E.; McNamura, M.; Mate, M.; Mecerreyes, D.; Benoit, D. G.; Hedrick, J. L.; Mansky, P.; Huang, E.; Russell, T. P.; Hawker, C. J. Controlled synthesis of polymer brushes by "living" free radical polymerization techniques. *Macromolecules* **1999**, *32*, 1424−1431.
(33) Kobayashi, M.; Terada, M.; Terayama, Y.; Kikuchi, M.; Takahara, A. Direct synthesis of well-defined poly[{2-(methacryloyloxy)ethyl}trimethyl ammonium chloride] brush via surface-initiated ATRP in fluoroalcohol. *Macromolecules* **2010**, *43*, 8409−8415.
(34) Yamaguchi, H.; Honda, K.; Kobayashi, M.; Morita, M.; Masunaga, H.; Sakata, O.; Sasaki, S.; Takahara, A. Molecular aggregation state of surface-grafted poly{2-(perfluorooctyl)ethyl acrylate} thin film analyzed by grazing incidence X-ray diffraction. *Polym. J.* **2008**, *40*, 854−860.
(35) Kobayashi, M.; Takahara, A. Synthesis and frictional properties of poly(2,3-dihydroxypropyl methacrylate) brush prepared by surface-initiated atom transfer radical polymerization. *Chem. Lett.* **2005**, *34*, 1582−1583.
(36) Terayama, Y.; Kobayashi, M.; Takahara, A. Preparation and surface properties of poly(vinyl alcohol) brush. *Chem. Lett.* **2007**, *36*, 1280−1281.
(37) Terayama, Y.; Kikuchi, M.; Kobayashi, M.; Takahara, A. Well-defined poly(sulfobetaine) brushes prepared by surface-Initiated ATRP using a fluoroalcohol and ionic liquids as the solvents. *Macromolecules* **2011**, *44*, 104−111.
(38) Tugulu, S.; Barbey, R.; Harms, M.; Fricke, M.; Volkmer, D.; Rossi, A.; Klok, H.-A. Synthesis of poly(methacrylic acid) brushes via surface-initiated atom transfer radical polymerization of sodium methacrylate and their use as substrates for the mineralization of calcium carbonate. *Macromolecules* **2007**, *40*, 168−177.
(39) Masci, G.; Bontempo, D.; Tiso, N.; Diociaiuti, M.; Mannina, L.; Capitani, D.; Crescenzi, V. Atom transfer radical polymerization of potassium 3-sulfopropyl methacrylate: direct synthesis of amphiphilic block copolymers with methyl methacrylate. *Macromolecules* **2004**, *37*, 4464−4473.
(40) Extrand, C. W.; Kumagai, Y. An experimental study of contact angle hysteresis. *J. Colloid Interface Sci.* **1997**, *191*, 378−383.
(41) Huang, X.; Wirth, M. J. Surface initiation of living radical polymerization for growth of tethered chains of low polydispersity. *Macromolecules* **1999**, *32*, 1694−1696.
(42) Blomberg, S.; Ostberg, S.; Harth, E.; Bosman, A. W.; van Horn, B.; Hawker, C. J. Production of crosslinked, hollow nanoparticles by surface-initiated living free-radical polymerization. *J. Polym. Sci., Part A: Polym. Chem.* **2002**, *40*, 1309−1320.
(43) van OSS, C. J. Surface Tension Components and Parameters of Liquids and Solids. *Interfacial Forces in Aqueous Media*; Marcel Dekker: New York, 1994; pp 170−185.
(44) van OSS, C. J.; Ju, L.; Chaudhury, M. K.; Good, R. J. Estimation of the polar parameters of the surface tension of liquids by contact angle measurements on gels. *J. Colloid Interface Sci.* **1989**, *128*, 313−319.
(45) Jasper, J. J. The surface tension of pure liquid compound. *J. Phys. Chem. Ref. Data* **1972**, *1*, 841−1009.
(46) van Oss, C. J.; Roberts, M. J.; Good, R. J.; Chaudhury, M. K. Determination of the apolar component of the surface tension of water by contact angle measurements on gels. *Colloids Surf.* **1987**, *23*, 369−373.
(47) Pittman, A. G. In *Fluoropolymers*; Wall, L. A., Ed.; Wiley-Interscience: New York, 1972; pp 419.
(48) Honda, K.; Morita, M.; Otsuka, H.; Takahara, A. Molecular aggregation structure and surface properties of poly(fluoroalkyl acrylate) thin films. *Macromolecules* **2005**, *38*, 5699−5705.
(49) Honda, K.; Yakabe, H.; Koga, T.; Sasaki, S.; Sakata, O.; Otsuka, H.; Takahara, A. Molecular aggregation structure of poly(fluoroalkyl acrylate) thin films evaluated by synchrotron-sourced grazing-incidence X-ray diffraction. *Chem. Lett.* **2005**, *34*, 1024−1025.
(50) Honda, K.; Yamaguchi, H.; Kobayashi, M.; Morita, M.; Takahara, A. Surface molecular aggregation structure and surface physicochemical properties of poly(fluoroalkyl acrylate) thin films. *J. Phys.: Conf. Ser.* **2008**, *100*, 012035.
(51) Honda, K.; Morita, M.; Masunaga, H.; Sasaki, S.; Takata, M.; Takahara, A. Room-temperature nanoimprint lithography for crystalline poly(fluoroalkyl acrylate) thin films. *Soft Matter* **2010**, *6*, 870−875.
(52) Yamaguchi, H.; Kikuchi, M.; Kobayashi, M.; Ogawa, H.; Masunaga, H.; Sakata, O.; Takahara, A. Influence of molecular weight dispersity of poly{2-(perfluorooctyl)ethyl acrylate} brushes on their molecular aggregation states and wetting behavior. *Macromolecules* **2012**, *45*, 1509−1516.
(53) Andrade, J. D.; Ma, S. M.; King, R. N.; Dregonis, D. E. Contact angles at the solid-water interface. *J. Colloid Interface Sci.* **1979**, *72*, 488−494.
(54) Andrade, J. D.; Chen, W. Y. Probing polymer surface and interface dynamics. *Surf. Interface Anal.* **1986**, *8*, 253−256.
(55) Tingey, T. G.; Andrade, J. D. Probing surface micro-heterogeneity of poly(ether urethanes) in an aqueous environment. *Langmuir* **1991**, *7*, 2471−2478.
(56) Busscher, H. J.; Van Pelt, A. W. J.; De Boer, P.; De Jong, H. P.; Arends, J. The effect of surface roughening of polymers on measured contact angles of liquids. *Colloids Surf.* **1984**, *9*, 319−331.
(57) Rangwalla, H.; Schwab, A. D.; Yurdumakan, B.; Yablon, D. G.; Yeganeh, M. S.; Dhinojwala, A. Molecular structure of an alkyl-side-chain polymer-water interface: origins of contact angle hysteresis. *Langmuir* **2004**, *20*, 8625−8633.
(58) Extrand, C. W. Contact angles and hysteresis on surfaces with chemically heterogeneous islands. *Langmuir* **2003**, *19*, 3793−3796.
(59) Wang, L.; Wei, J.; Su, Z. Fabrication of surfaces with extremely high contact angle hysteresis from polyelectrolyte multilayer. *Langmuir* **2011**, *27*, 15299−15304.
(60) Cohen Stuart, M. A.; de Vos, W. M.; Leermakers, G. A. M. Why surfaces modified by flexible polymers often have a finite contact angle for good solvents. *Langmuir* **2006**, *22*, 1722−1728.
(61) Muller, P.; Sudre, G.; Théodoly, O. Wetting transition on hydrophobic surfaces covered by polyelectrolyte brushes. *Langmuir* **2008**, *24*, 9541−9550.
(62) Hamilton, W. C. A technique for the characterization of hydrophilic solid surfaces. *J. Colloid Interface Sci.* **1972**, *40*, 219−222.

(63) Nakamae, K.; Miyata, T.; Ootsuki, N. Evaluation of surface characteristics of polymers in water. Measurement of surface free energy in water. *Makromol. Chem. Rapid Commun.* **1993**, *14*, 413−420.
(64) Andrade, J. D.; King, R. N.; Gregonis, D. E.; Coleman, D. L. Surface characterization of poly(hydroxyethyl methacrylate) and related polymers. I. Contact angle methods in water. *J. Polym. Sci., Polym. Symp.* **1979**, *66*, 313−336.
(65) Fowkes, F. M. Attractive forces at interfaces. *Ind. Eng. Chem.* **1964**, *56*, 40−52.
(66) Tamai, Y.; Makuuchi, K.; Suzuki, M. Experimental analysis of interfacial forces at the plane surface of solids. *J. Phys. Chem.* **1967**, *71*, 4176−4179.
(67) Schmidt, D. L.; Coburn, C. E.; Dekoven, B. M.; Potter, G. E.; Meyers, G. F.; Fischer, D. A. Water-based non-stick hydrophobic coatings. *Nature* **1994**, *368*, 39−41.
(68) Comyn, J. Contact angles and adhesive bondings. *Int. J. Adhes. Adhes.* **1992**, *12*, 145−149.
(69) Clint, J. H.; Wicks, A. C. Adhesion under water: surface energy considerations. *Int. J. Adhes. Adhes.* **2001**, *21*, 267−273.
(70) Clint, J. H. Adhesion and components of solid surface energies. *Curr. Opin. Colloid Interface Sci.* **2001**, *6*, 28−33.
(71) Andreas, J. M.; Hauser, E. A.; Tucker, W. B. Boundary tension by pendant drops. *J. Phys. Chem.* **1938**, *42*, 1001−1019.
(72) Schulz, D. N.; Peiffer, D. G.; Agarwal, P. K.; Larabee, J.; Kaladas, J. J.; Soni, L.; Handwerker, B.; Garner, R. T. Phase behaviour and solution properties of sulphobetaine polymers. *Polymer* **1986**, *27*, 1734−1742.
(73) Kikuchi, M.; Terayama, Y.; Hoshino, T.; Kobayashi, M.; Ogawa, H.; Masunaga, H.; Takahara, A. Static and dynamic scattering from polysulfobetaine immobilized on silica nanoparticle in ionic liquid. *J. Phys.: Conf. Ser.* **2011**, *272*, 012016.
(74) Kikuchi, M.; Terayama, Y.; Ishikawa, T.; Hoshino, T.; Kobayashi, M.; Ogawa, H.; Masunaga, H.; Koike, J.; Horigome, M.; Ishihara, K.; Takahara, A. Chain dimension of polyampholytes in solution and immobilized brush states. *Polym. J.* **2012**, *44*, 121−130.
(75) Terayama, Y.; Arita, H.; Ishikawa, T.; Kikuchi, M.; Mitamura, K.; Kobayashi, M.; Yamada, N. L.; Takahara, A. Chain dimensions in free and immobilized brush states of polysulfobetaine in aqueous solution at various salt concentrations. *J. Phys.: Conf. Ser.* **2011**, *272*, 012010.
(76) Yang, R.; Xu, J.; Ozaydin-Ince, G.; Wong, S. Y.; Gleason, K. K. Surface-tethered zwitterionic ultrathin antifouling coatings on reverse osmosis membranes by initiated chemical vapor deposition. *Chem. Mater.* **2011**, *23*, 1263−1272.

View Article Online / Journal Homepage / Table of Contents for this issue
Dynamic Article Links

Soft Matter

Cite this: *Soft Matter*, 2012, **8**, 5477

www.rsc.org/softmatter

PAPER

Designing dynamic surfaces for regulation of biological responses†

Ji-Hun Seo,[ad] Sachiro Kakinoki,[bd] Yuuki Inoue,[cd] Tetsuji Yamaoka,[bd] Kazuhiko Ishihara[cd] and Nobuhiko Yui*[ad]

Received 12th February 2012, Accepted 5th March 2012
DOI: 10.1039/c2sm25318f

ABA block copolymers composed of highly methylated polyrotaxane and hydrophobic anchoring terminal segments containing 2-methacryloyloxyethyl phosphorylcholine (MPC) and *n*-butyl methacrylate (PMB) (OMe-PRX-PMB) were synthesized as a platform of molecularly dynamic biomaterials. A contact angle measurement indicated that polymer surfaces with higher molecular mobility factors (M_f) estimated from quartz crystal microbalance with dissipation (QCM-D) measurements showed more significant changes in hydrophilicity in response to an environmental change between air and water; the OMe-PRX-PMB surface showed the highest M_f among the prepared polymer surfaces. Fibrinogen adsorption and its conformational analysis estimated by QCM-D and enzyme-linked immunosorbent assay revealed that large amounts of fibrinogen adsorption occurred in a soft manner on the OMe-PRX-PMB surface and that the antibody binding to the C-terminus of the fibrinogen γ chains responsible for platelet adhesion and activation decreased as the M_f value increased. Furthermore, it was found that the OMe-PRX-PMB surface showed low platelet adhesion and high fibroblast adhesion, suggesting that molecular movement on biomaterial surfaces could be one of the key parameters in the regulation of a non-specific biological response.

1. Introduction

When artificial materials are placed in a biological environment, protein–material interaction primarily occurs on the surfaces along with the physicochemical properties of materials.[1–3] The state of adsorbed proteins plays a dominant role in most non-specific biological responses such as foreign body reaction or clot formation.[4] Therefore, the development of anti-fouling materials that are able to prevent non-specific protein interaction has been a critical issue in the field of biomaterials for the last several decades.[5] Although several applications of anti-fouling materials have been reported for the limited number of available biomaterials such as artificial blood vessels, anti-fouling properties also prevent the promotion of tissue regeneration on the materials implanted in a damaged body. Because the extracellular matrix composed of protein molecules is an essential factor for cell adhesion and tissue formation, protein adsorption on the biomaterials is a fundamental requirement.[6] However, non-specifically adsorbed surface proteins also can trigger undesirable biological reactions as mentioned above. This paradoxical problem of protein adsorption has been a fundamental barrier to the development of ideal biomaterials that prohibit non-specific biological reactions as well as promote specific cell adhesion. Because conformational change of adsorbed proteins is the cause of most biological responses on the artificial materials, it is important to regulate protein conformation in the design of ideal biomaterials. A number of variables that have an effect on the conformational change of adsorbed proteins have been reported in the last several decades. These include polarity, charge density, and other geometrical factors such as surface roughness.[7–9] Nowadays, these factors are commonly used to regulate biological responses on artificial materials. However, to the best of our knowledge, there have been no reports on key variables responsible for moderate conformational change that can modulate cell adhesion for tissue regeneration and prevent undesirable foreign body reactions such as blood clotting and inflammatory reaction. Not only dynamic cell membranes but also single protein molecules continuously move on the surface of artificial materials until they determine the thermodynamic standpoint for final conformations.[10] Therefore, even well-defined artificial materials with determined surface properties could not withstand the dynamic responses of the biological environment. We presume that rigid material surfaces with a determined surface nature generate conformational changes in adsorbed proteins, and finally trigger undesirable biological responses. Therefore, in this paper, we present a novel concept, which proposes that dynamic material surfaces that flexibly respond to a dynamic biological environment can possibly overcome the limitations of traditional biomaterials.

[a]*Institute of Biomaterials and Bioengineering, Tokyo Medical and Dental University, Tokyo 101-0062, Japan. E-mail: yui.org@tmd.ac.jp; Fax: +81-3-5280-8027; Tel: +81-3-5280-8020*
[b]*Department of Biomedical Engineering, National Cerebral and Cardiovascular Center Research Institute, Suita, Osaka, 565-8565, Japan*
[c]*Department of Materials Engineering, The University of Tokyo, Tokyo 113-8656, Japan*
[d]*JST-CREST, Tokyo 102-0076, Japan*
† Electronic supplementary information (ESI) available: NMR and AFM images. See DOI: 10.1039/c2sm25318f

Polyrotaxane (PRX) is a representative molecular assembly consisting of a host molecule, *e.g.*, α-cyclodextrin (α-CD), threading a guest molecule, *e.g.*, linear polyethylene glycol (PEG). Because both components are not covalently connected, the threaded α-CD molecules are anticipated to be movable along the PEG backbone. Based on this perspective, we have systematically studied the effect of the molecular mobility of polyrotaxanes on biological interaction with proteins. Throughout these studies, we clarified that CD mobility is influential in enhancing multivalent interaction with receptor proteins in biological ligand-immobilized polyrotaxanes.[11–15] Furthermore, we have demonstrated that cytocleavable polyrotaxanes are very effective in DNA delivery to the nucleus in a target cell.[16–21] As polymeric materials for designing movable surfaces using a polyrotaxane structure, the block copolymer containing the PRX segment was previously synthesized by using an atom transfer radical polymerization method with hydrophobic isobutyl methacrylate.[22] The prepared surface showed high molecular mobility and eliminated adsorption of human plasma fibrinogen by introducing a low degree of methoxy (OMe) groups of α-CD molecules on the PRX segment. In this study, we introduced bio-inert poly((2-methacryloyloxyethyl phosphorylcholine)-co-(*n*-butyl methacrylate)) (PMB) anchoring terminals at both ends of the PRX segment by using the reversible addition-fragmentation chain transfer (RAFT) polymerization method. Furthermore, a higher degree of OMe groups were introduced to each threaded α-CD molecule to modulate the protein interaction on the hydrophilic PRX moiety. The aim of this study is to investigate the dynamic interaction of mobile OMe groups with protein molecules and the associated biological responses including platelet and fibroblast adhesion.

2. Materials and methods

2.1 Materials

A 2-methacryloyloxyethyl phosphorylcholine (MPC) was obtained from NOF Co. (Tokyo, Japan). 4-(Benzodithioyl)-4-cyanopentanoic acid (CTA) was synthesized according to a previously reported method.[23] α-CD, BMA, sodium hydride, iodomethane, α,α′-azobisisobutyronitrile (AIBN), and all the organic solvents were purchased from Tokyo Kasei Co. (Tokyo, Japan) and used as received. PEG (number average molecular weight of 20 kDa) (PEG 20k) was purchased from the Sigma-Aldrich Chemical Co. (St. Louis, MO, USA), and the hydroxyl end groups were converted to amine groups by using a previously reported method.[24]

Goat polyclonal antibody to mouse IgG conjugated with horseradish peroxidase (HRP) and anti-fibrinogen alpha antibody (49D2) were purchased from Abcam Inc. (Cambridge, MA, USA), and anti-fibrinogen gamma antibody (clone2 G2. H9) was purchased from Millipore (Bedford, MA, USA). Human plasma fibrinogen was purchased from Sigma-Aldrich (St. Louis, MO, USA) and other biological reagents were purchased from Gibco Invitrogen Corp. (Grand Island, NY, USA).

Fresh blood was donated by a healthy human volunteer at the National Cerebral and Cardiovascular Center Research Institute. The whole blood was collected with 10 v/v% of 3.8% trisodium citrate solution, and platelet-rich plasma (PRP) was prepared *via* a centrifugation process (200 gravity, 15 min at 25 °C). After this, the PRP was further centrifuged (1500 gravity, 10 min at 25 °C) to obtain platelet-poor plasma (PPP). The number of platelets in the PRP was then adjusted by PPP to 1.0×10^7 mL^{-1}. The use of whole blood and platelets were approved by the Biosafety Committee at National Cerebral and Cardiovascular Center Research Institute.

2.2 Block copolymer synthesis

Synthesis of pseudo-PRX macro CTA. Previously, PEG 20k macro chain transfer agent (CTA) was synthesized as follows: 1 g of PEG 20k bis-amine (0.050 mmol), and 0.018 g of dimethylamino pyridine (0.15 mmol) were dissolved in 5 mL of dichloromethane. To this, 0.14 g of CTA (0.50 mmol) and 0.082 g of water soluble carbodiimide (0.50 mmol) were added and stirred for 12 h at room temperature. Next, some fresh dichloromethane was added and the mixture was re-precipitated in cold diethyl ether. The crude product was then dissolved in water, and the dialysis process was carried out (MWCO 3500) for a day, followed by the lyophilization process.

The obtained PEG macro-CTA (0.35 g) was then mixed with 3.5 g of α-CD in 25 mL of water at room temperature until the light-pink and turbid inclusion complex was formed. The precipitate was then isolated by means of the centrifuge process, and washed again with 25 mL of water, followed by a repeat of the centrifugation process. The precipitate was then freeze-dried to obtain pink-colored inclusion complex of pseudo-PRX macro CTA.

Synthesis of PRX-PMB block copolymer. A 0.600 g of pseudo-PRX macro-CTA was allowed to react with 0.354 g of MPC (1.20 mmol) and 0.633 g of BMA (4.45 mmol) monomer in 7 mL of ethanol–toluene (1 : 1) mixed solvent, by using 0.820 mg of AIBN (5.00 μmol) as an initiator. The heterogeneous solution was bubbled with an Ar atmosphere for 15 min prior to placement in a 60 °C oil bath. After 24 h, 15 mL of fresh mixed solvent was added to the solution and the precipitate was obtained by means of the centrifugation process. The obtained polymer was sequentially washed with ethanol, acetone, dimethyl sulfoxide (DMSO), and acetone to remove residual monomers and α-CD. The final precipitate was then dried at 40 °C *in vacuo* and the polymer was obtained as a white powder. A similar process was carried out to synthesize PMB and PEG-PMB by using CAT or PEG-CTA as a macro CTA.

Methylation of PRX-PMB block copolymer. 200 mg of the synthesized PRX-PMB block copolymer was heterogeneously dissolved in 7 mL of dehydrated DMSO. To this, 0.155 g of sodium hydride (6.3 mmol) was added under an Ar atmosphere and mixed for 30 min at room temperature. Next, 0.102 g of iodomethane (0.719 mmol) was slowly injected to the mixture and stirred for 3 h at room temperature. After the pH was neutralized with 6 N HCl solution, the mixture was transferred to a dialysis tube (MWCO0 : 20000) and the dialysis process was carried out for 3 days. The methylated PRX-PMB (OMe-PRX-PMB) block copolymer was then obtained by means of the lyophilization process.

2.3 Surface characteristics

The synthesized polymer (5 mg) was initially dispensed in 5 mL ethanol. After that, 5 mL of water was added to prepare 0.05 wt % of clear polymer solution. Each polymer solution (30 μL) was then uniformly cast on a Cell Desk™ (Sumitomo Bakelite Co., Japan), and dried in a clean box at room temperature for a day. Each polymer surface was stabilized in water for a day prior to the surface characterization and other biological evaluations.

X-ray photoelectron spectroscopy (XPS) was used to analyze the surface chemical elements by using a magnesium K_α source with a take-off angle of 90° (Kratos/Shimadzu, Kyoto, Japan). The characterized elements were C, N, and P and the binding energies were referenced to the C_{1s} peak at 285.0 eV.

The static water and air bubble contact angles were measured using a goniometer (Kyowa Interface Science Co., Tokyo, Japan). Prior to the measurement, the surface tension of water (72 mN m^{-1}) was confirmed by means of the pendant drop method using a Young–Laplace curve-fitting algorithm. Under dry conditions, 3 μL of water droplets were brought in contact with the polymer surface for 30 s, and the contact angles were measured using photographic images. Under wet conditions, 5 μL of air bubble was brought in contact with the surfaces in water, and the contact angles again were measured using photographic images.

Quartz crystal microbalance with dissipation (QCM-D) monitoring of the polymer surfaces was carried out by using Q-sense E1-HO (Meiwafosis Co., LTD, Tokyo, Japan). The molecular mobility at the hydrated surfaces was estimated as follows: the Au sensor was cleaned by applying an O_2 plasma treatment for 5 min and a sequential washing with acetone and ethanol, and dried with Ar blowing. The sensor was placed in an open-type chamber equipped with the QCM-D apparatus at 25 °C. The resonance frequency at 35 MHz ($f_{gold,\ dry}$) and the dissipation energy ($D_{gold,\ dry}$) was then measured. Subsequently, $f_{gold,\ wet}$ and $D_{gold,\ wet}$ in a hydrated state were measured with the bare gold in contact with pure water. After the water was removed from each polymer solution and dried by using a stream of air, 20 mL of it was dropped on the surface. After the surface was dried, the resonance frequencies ($f_{sample,\ dry}$ and $f_{sample,\ wet}$) and dissipation energies ($D_{sample,\ dry}$ and $D_{sample,\ wet}$) of the coated surface in both the dry and hydrated states were measured using the same procedure as above.[22]

2.4 Evaluation of biological responses to the block copolymer surface

Protein adsorption test. The polymer-cast Cell Desk™ was immersed in a 0.3 mg mL^{-1} of fibrinogen solution or 10% human plasma in phosphate buffered saline (PBS, pH 7.4) for 1 h at 37 °C. Next, the samples were rinsed twice with 500 mL of fresh PBS employing the stirring method (300 rpm for 5 min). The adsorbed protein was detached in sodium dodecyl sulfate (SDS, 1 wt% in water) by sonication for 20 min, and the protein concentration in the SDS solution was determined by means of the micro-BCA™ method.

The state of adsorbed fibrinogen was also analyzed by QCM-D measurements. The Au substrate was cast with each polymer solution, and the energy dissipation factor (D) and frequency (f) were stabilized under a flow of PBS (0.1 mL min^{-1}). Then, a 0.3 mg mL^{-1} fibrinogen solution was flowed for 1 h, and fresh PBS was flowed for another 1 h. Each D and f value was continuously monitored during the whole process of protein adsorption. The amount of adsorbed proteins was calculated by using the simplified Sauerbrey equation with an overtone value of 7 and C = 17.7 ng cm^{-2}, as follows:[25]

$$\Delta m = -C\Delta f/n$$

An enzyme-linked immunosorbent assay (ELISA) was carried out to estimate the conformational change of adsorbed fibrinogen as follows: initially, each polymer surface was brought in contact with whole human plasma for 5 min at 37 °C. After rinsing three times with PBS, each sample was brought in contact with 2 μg mL^{-1} of the primary antibody (anti-fibrinogen alpha or gamma) solution for 1 h at room temperature. After rinsing four times with PBS, samples were allowed to react with 8 μg mL^{-1} of the secondary antibody conjugated with HRP in bovine serum albumin (BSA) pre-treated 24 well plates for 2 h. After rinsing six times with PBS-T, 0.5 mL of solution (mixture of 10 mL guanylic acid buffer (pH 3.3), 0.125 mL of 3,3′,5,5′-tetramethylbenzidine (44 mM), and 0.018 mL of H_2O_2) was added to each sample surface in the BSA pre-treated well. After the reaction was quenched with 2 N of sulfuric acid, the absorbance at 450 nm in each resulting solution was measured by a micro plate reader (Multiskan FC, Thermo Fisher Scientific, St. Herblain, France).

Each polymer surface was brought in contact with 500 μL of PRP in a 24 well plate at 37 °C for 2 h. After rinsing three times with fresh PBS, platelet adhesion was quantitatively analyzed by means of lactate dehydrogenase (LDH) assay, and the morphology of adhering platelets was observed using a fluorescent microscope after dying F-actin with rhodamine conjugated phalloidin.[26]

The cell adhesion test using NIH3T3 mouse fibroblast was performed on each polymer surface. Approximately 1.0 × 10^5 cells in 1.0 mL of minimum essential medium (Invitrogen Corp., Carlsbad, CA, USA) supplemented by 10% fetal bovine serum was incubated on polymer surfaces for 6 h. After rinsing with fresh medium, the surface adhering cells were observed using an optical microscope and the number of adhering cells was counted by a Cell Counting Kit #8 (Dojindo, Tokyo, Japan).

3. Results and discussion

3.1 Preparation of PRX block copolymers

Scheme 1 shows the overall concept of this study in preparing molecularly dynamic surfaces for evaluating biological

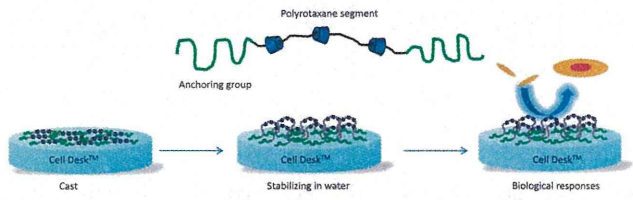

Scheme 1 Schematic explanation of development of dynamic surface.

responses. To develop dynamic surfaces, PRX segments are necessary to be combined with hydrophobic anchoring terminal segments at both ends. Here, a random copolymer segment composed of MPC and BMA (PMB) was selected as an anchoring terminal (Fig. 1). The PMB segment is a well-known coating unit that can be stably immobilized on a hydrophobic material's surface to prevent non-specific biological responses.[27] To synthesize the PRX block copolymer, RAFT chain transfer agent (CTA) was initially introduced to PEG-bisamine, and pseudo-PRX macro CTA was synthesized with α-CD. Subsequently, MPC and BMA were introduced *via* the RAFT polymerization method. Then, the hydrophobic OMe group was introduced to each hydroxyl group of the α-CD molecules. As a result, around 90% of the hydroxyl groups were successfully substituted by OMe groups. Fig. 2 shows the ^{1}H-NMR and FT-IR results of the synthesized OMe-PRX-PMB. Obviously, a strong OMe peak was observed at 3.2 and 3.3 ppm, which does not exist in PRX-PMB (Figure S3†). All the functional groups containing MPC units were successfully confirmed by combination of ^{1}H-NMR and FT-IR results. The detailed molecular profiles are summarized in Table 1.

3.2 Surface characterization of PRX block copolymer

The prepared polymer surfaces cast on the Cell Desk™ were analyzed by XPS. In all the cases of polymer surfaces, characteristic N_{1s} and P_{2p} signals from the PMB segment appeared at 402.5 eV and 134.0 eV, respectively, whereas the characteristic peak of the Cell Desk™ surface at 290 eV C_{1s} had disappeared (Fig. 3). This result indicates that all the polymer samples are uniformly prepared on the Cell Desk™ surface by means of the simple solvent cast method. Throughout an ellipsometry measurement, it was confirmed that all the polymer films were formed within a thickness of 20~30 nm (data not shown). In any case, it was confirmed that all the polymers were stably cast on the overall Cell Desk™ surface by anchoring the PMB segment.

The wettability of the prepared polymer surfaces was estimated in both air and water using water droplets and air bubbles, respectively. The contact angles of the air bubbles on the PMB, PRX-PMB, and OMe-PRX-PMB surfaces were not measured, because the air bubbles were rolling on these surfaces. These findings indicate that the surfaces are extremely hydrophilic in an aqueous environment and the contact angles are close to 0°. The contact angle hysteresis along with an air–water environmental change was indirectly measured by comparing both results (Fig. 4). The PMB surface showed a slightly higher contact angle hysteresis (~40°) than that of the Cell Desk™, which is possibly due to the increased directionality of the hydrophilic phosphorylcholine group in the water compared to the state in the air as previously reported.[28] The PEG-PMB and PRX-PMB surfaces showed a contact angle hysteresis of around 60°. It is thought that the swelling of the hydrophilic PEG and PRX segments of the block copolymer in the water was contributing to the slight increase of the contact angle hysteresis in addition to the directionality effect of the PMB segment. In contrast to the moderate hysteresis changes in these control samples, the OMe-PRX-PMB surface showed a contact angle hysteresis of around 100°. This indicates that the surface property of the OMe-PRX-PMB has drastically changed in response to the environmental change between air and water. The smoothness of all the surfaces was confirmed by atomic force microscope measurement, suggesting that the effect of surface roughness on the contact angle hysteresis should be negligible (Figure S4†). Even though more supporting information is required, we speculate that this dynamic change in the surface property is due to the dynamic movement of CD molecules on the PEG backbone.

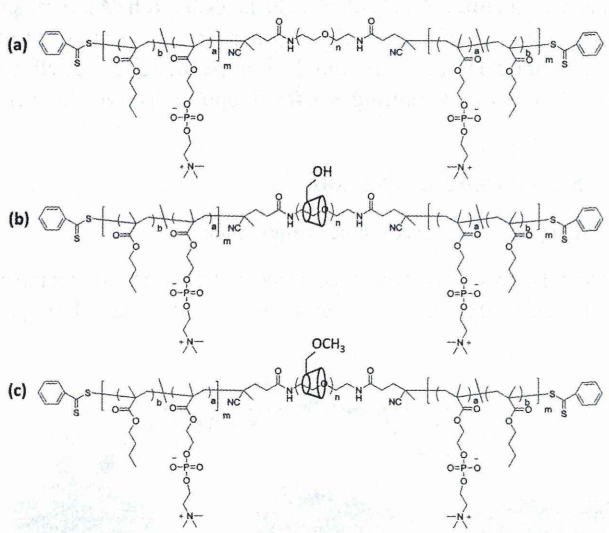

Fig. 1 Molecular structure of (a) PEG-PMB, (b) PRX-PMB, and (c) OMe-PRX-PMB.

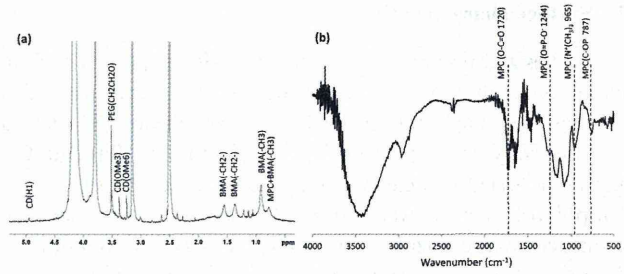

Fig. 2 (a) ^{1}H NMR (DMSO-d_6:MeOD = 1 : 1) and (b) FT-IR spectra of OMe-PRX-PMB.

To estimate the dynamic nature of the prepared PRX block copolymers in more detail, the surface dynamics in an aqueous media were estimated by the QCM-D measurement method as previously reported.[22] Generally, the energy dissipation value on a materials surface (ΔD) is directly related to the viscoelasticity of the materials adsorbed on an Au surface. When highly mobile surface elements such as tethering polymer chains or weakly cross-linked hydrogels exist, ΔD values drastically increase against rigid surfaces. This viscoelasticity of the surface could be interpreted as one of the parameters that indicate dynamic molecular movement of the surfaces. To consider the effect of the amount of polymers, each ΔD value was normalized to its adsorption mass related factor (Δf) using the following equation:

$$\text{Surface mobility factor } (M_f) = (D_{\text{sample, wet}} - D_{\text{gold, wet}})/(f_{\text{gold, dry}} - f_{\text{sample, dry}})$$

Table 1 Molecular profile of the synthesized polymers (^{1}H NMR)

	MPC (mol% in PMB)	BMA (mol% in PMB)	PEG (weight %)	Number of CD per PEG chain
Cell Desk™	0	0	0	0
PMB	19	81	0	0
PEG-PMB	23	77	24	0
PRX-PMB	12	88	23	12
OMe-PRX-PMB	12	88	23	12 methylation >90%

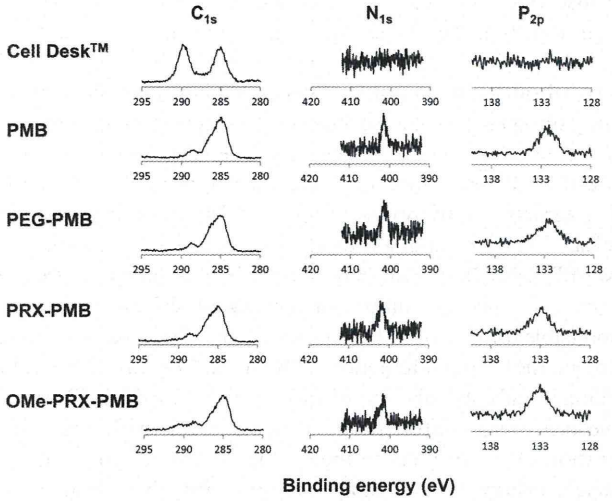

Fig. 3 XPS profile of cast polymer surfaces.

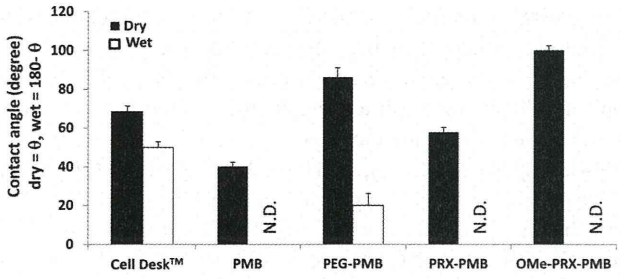

Fig. 4 Contact angles measured by water droplet in air and air bubble in water (n = 3).

Fig. 5 (a) shows the resulting value of M_f on each prepared polymer surface. The PEG-PMB showed a slightly higher M_f value than PMB. This is possibly due to the chain mobility of the hydrated loop-type PEG segment in the middle of the block copolymer. The OMe-PRX-PMB surface showed the highest M_f value among the prepared polymer surfaces, suggesting that the OMe group-containing the PRX segment exhibits the highest molecular mobility in an aqueous media. The lower M_f value on the PRX-PMB surface compared to those on the PEG-PMB and OMe-PRX-PMB surfaces is thought to be caused by the rigid crystalline formation of the CD molecules by intermolecular hydrogen bonding that interferes with the mobility of the PEG backbone. In any event, it was confirmed that the OMe-PRX-PMB surface exhibits the highest surface viscoelasticity—possibly induced by the dynamic molecular mobility on the surface—compared to other control polymer surfaces. Of special interest is the plot of the contact angle hysteresis along with the M_f value (Fig. 5 (b)). It is obvious that the relationship between the contact angle hysteresis and the M_f value is straightforward. This finding suggests that the dynamic change of surface wettability in response to the environmental change, is strongly governed by the molecular mobility on the surface.

3.3 Non-specific protein interaction with PRX block copolymer surfaces

Fig. 6 (a) shows the result of the human fibrinogen adsorption test. As expected, hydrophilic control samples (PMB, PEG-PMB, and PRX-PMB surfaces) showed relatively low fibrinogen adsorption. Similar results were also confirmed in the case of the

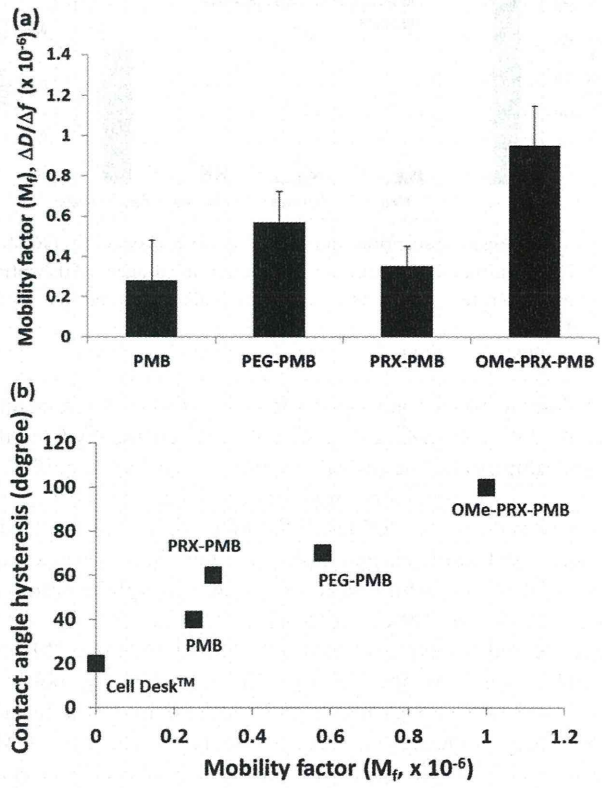

Fig. 5 (a) Result of M_f estimated from QCM-D and (b) plot of contact angle hysteresis *versus* M_f values (n = 3). The contact angle hysteresis was calculated by subtracting the contact angle of the water droplet in the air from that of the air bubble in the water bubble in water (n = 3).

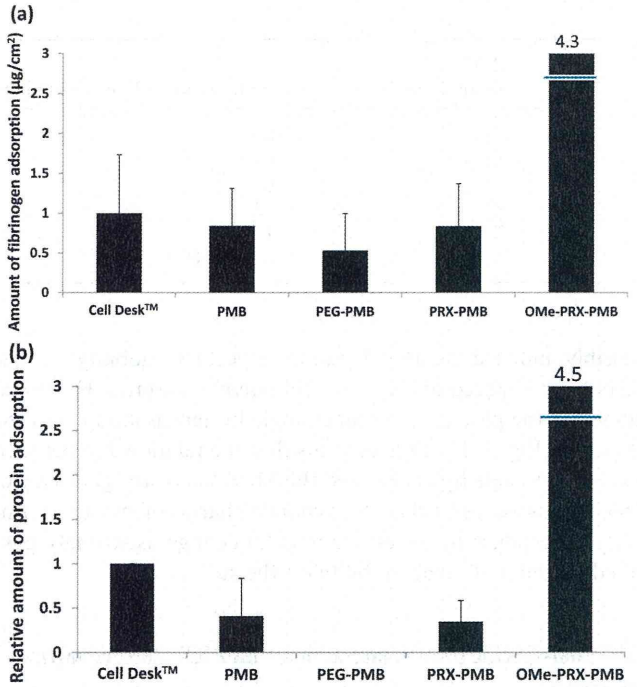

Fig. 6 Protein adsorption measured by micro-BCA™ method using (a) human fibrinogen at 10% plasma concentration and (b) 10% human PPP (n = 3).

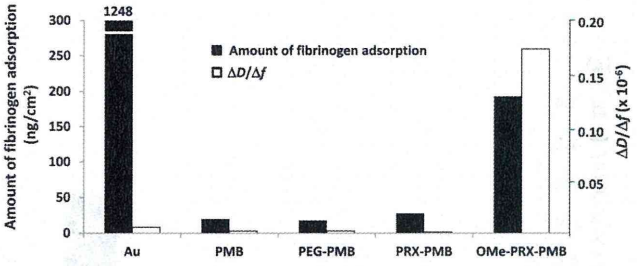

Fig. 7 Fibrinogen adsorption and $\Delta D/\Delta f$ value measured by QCM-D using 10% plasma concentration of human fibrinogen. Adsorption condition: flow rate = 0.1 mL min^{-1}, 1 h protein flow followed by 1 h PBS flow (pH 7.4).

whole human plasma adsorption test (Fig. 6 (b)). These results indicate that non-specific interaction between the hydrophilic control samples and the plasma protein was not very significant. In contrast, a significantly large amount of protein adsorption was observed on the OMe-PRX-PMB surface in both the fibrinogen and whole plasma adsorption test. Because the OMe-PRX-PMB surface exhibited an extremely hydrophilic nature in water (Fig. 4), the surface hydrophilicity in an aqueous environment could not explain this result. Even though the OMe are hydrophobic groups, they along with the rest of the polymer provide adequate enough hydrogen bonding to make the surface appear hydrophilic in aqueous media. However, these OMe groups exposed on the outermost surface still allow for contact with plasma proteins which leads to protein binding and accumulation.

To understand the state of the adsorbed proteins more clearly, fibrinogen adsorption was carried out by means of QCM-D under the flow adsorption condition. As a result, the adsorption behavior similar to that of micro-BCA™ was further confirmed on all the polymer surfaces (Fig. 7). In particular, a significantly large amount of fibrinogen adsorption was observed only on the hydrophobic Au and OMe-PRX-PMB surfaces. However, it is noteworthy that the state of adsorbed fibrinogen was quite different between the bare Au and OMe-PRX-PMB surfaces. In the case of the bare Au surface, the adsorbed fibrinogen molecules showed a very low $\Delta D/\Delta f$ value, which indicates that the state of the adsorbed fibrinogen molecules is very rigid because the interaction with the Au surface is quite strong. In contrast, the adsorbed fibrinogen on the OMe-PRX-PMB surface showed a significantly higher $\Delta D/\Delta f$ value. This indicates that the energy dissipation of the adsorbed fibrinogen molecules along with the micro-vibration of the substrates is quite high. This phenomenon is only observed when adsorbed substances weakly interact with the surface; that is, fibrinogen molecules are adsorbed on the OMe-PRX-PMB surface in quite a soft manner. Why this kind of soft interaction only occurred on the OMe-PRX surface is still unclear. However, taking into account the dynamic nature of the OMe-PRX-PMB surface (Fig. 4 and 5), it is plausible that the dynamically movable nature of the OMe-PRX-PMB surface is responsible for the soft interaction with the fibrinogen molecules. Namely, the strong interaction with the surface was disturbed by dynamic mobility of the surface, thus, adsorbed fibrinogen molecules were continuously vibrating along with the micro-vibration of the surfaces to induce high-energy dissipation.

The conformational change of adsorbed fibrinogen on the dynamic polymer surfaces was estimated by means of the ELISA test using two types of primary antibodies, 49D2 and clone2 G2. H9, which can specifically bind to the N-terminus of the α-chain (1–16 peptide sequence) and the C-terminus of the γ-chain (434–453 peptide sequence) of the adsorbed fibrinogen, respectively. Fibrinogen molecules have two specific binding motifs responsible for cellular adhesion and aggregation. One is the dodecapeptide sequence existing close to the C-terminus of the γ-chain (400–411 peptide sequence), which is a binding site to GPIIb/IIIa on the platelet to finally trigger the activation of the platelet.[29] The other motif consists of the two RGD sequences in the α-chain (RGDF and RGDS on 95–98 and 572–575 peptide sequence), which is a binding site to the GPIIb/IIIa of the platelets as well as the $\alpha_v\beta_3$ integrin on various cells.[30] Previous ELISA studies on the adsorbed fibrinogen on polymer surfaces demonstrated that the surface presentation of the dodecapeptide sequence in adsorbed fibrinogen on material surfaces was well correlated with platelet adhesion whereas the relation of the presentation of the RGD motifs with the platelet adhesion was not so clear.[31,32] These results indicate that the C-terminus of the γ-chain, presenting the dodecapeptide sequence in the fibrinogen, is essential to induce the platelet-fibrinogen interaction, and the N-terminus of the α-chain itself does not seem to have a significant effect on the platelet adhesion. Therefore, it is considered that the exposure level of the C-terminus of the γ-chain is a good parameter to estimate the potency of the platelet adhesion. Therefore, how well the appearance of the platelet GPIIb/IIIa binding site in the C-terminus γ chain is suppressed could be a key to the development of ideal blood-contacting materials. Fig. 8 (a) shows the quantitative result of the secondary antibody binding specifically to the primary antibody

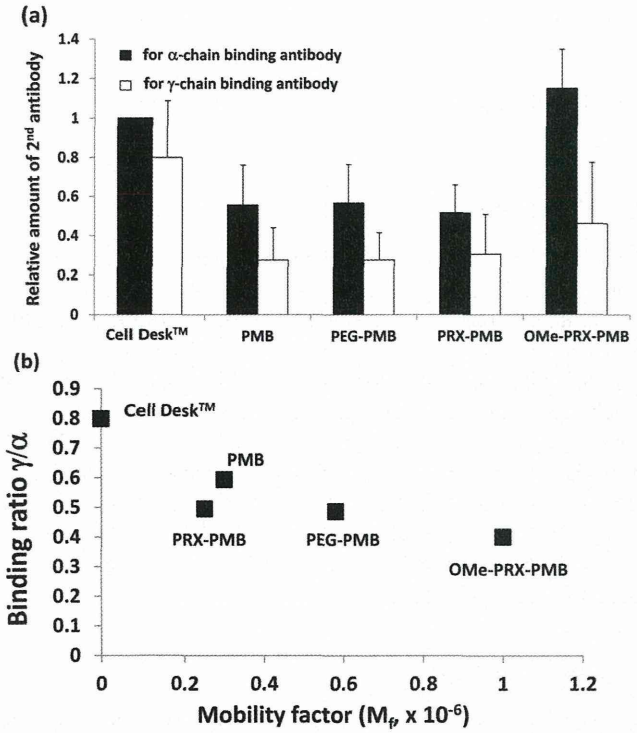

Fig. 8 (a) Relative amount of secondary antibody to the specific binding primary antibody on N-terminus α- and C-terminus γ-chains of adsorbed fibrinogen estimated by ELISA assay (n = 6) and (b) plot of γ : α binding ratio *versus* M_f values. Protein adsorption was carried out with 10% human plasma for 5 min contact prior to the ELISA test. The amount of secondary antibody was normalized to the amount of α-chain binding on the Cell Desk™.

bound to fibrinogen molecules. In the case of the Cell Desk™ surface, the amount of the binding antibody on both the γ- and α-chains was higher than that for other hydrophilic polymer surfaces, which indicates that the fibrinogen bound to the Cell Desk™ surface readily exposes both specific binding motifs. In contrast, other hydrophilic polymer surfaces showed a significantly lower level of the antibody binding in both the γ- and α-chains. This is possibly due to the quantitatively low level of adsorbed proteins as confirmed in the micro-BCA™ and QCM-D results. However, fibrinogen molecules on the OMe-PRX-PMB surface showed a quite interesting tendency. In spite of the significant amount of adsorbed plasma protein and fibrinogen, the amount of the secondary antibody for the C-terminus γ-chain binding antibody on the OMe-PRX-PMB surface was at a quite a low level compared to that on the Cell Desk™ surface (Figure S5†). This result suggests the possibility that inconsistent antibody binding was occurred due to the dynamic conformations which was induced by molecularly mobile segments in OMe-PRX-PMB. Fig. 8 (b) shows the plot of the antibody binding ratio (C-terminus γ-chain binding to N-terminus α-chain binding) *versus* the M_f values. It is obvious that the C-terminus γ-chain binding ratio compared to that of the N-terminus α-chain, decreased as the M_f value increased. Therefore, it is thought that the molecularly dynamic surfaces with high $\Delta D/\Delta f$ can induce moderate conformational changes no matter how many proteins are adsorbed on the surface.

3.4 Cellular responses to the PRX block copolymer surfaces

To estimate the effect of adsorbed plasma proteins on the biological responses, platelet and fibroblast adhesion tests were carried out by using the human PRP and NIH3T3 fibroblast. Fig. 9 (a) shows the result of platelet adhesion on the prepared polymer surfaces. Obviously, the Cell Desk™ surface induced large amounts of platelet adhesion on its surface, suggesting that the platelet adhesion is derived from a significant conformational change of the adsorbed proteins, including fibrinogen as confirmed by ELISA. In contrast, an insignificant number of adhering platelets was observed on all the prepared polymer surfaces. Fig. 9 (b) shows the quantitative result of adhering platelets along with the relative amount of the C-terminus γ-chain binding antibody. The resulting platelet adhesion was increased when the expression of the C-terminus γ-chain of the adsorbed fibrinogen was increased. This almost straightforward relationship is consistent with previously reported results.[31,32] The OMe-PRX-PMB surface showed a similar level of platelet adhesion in spite of the significant amount of adsorbed fibrinogen confirmed in the micro-BCA™ and QCM-D analyses. Several publications have stated that platelet adhesion normally increases in proportion to the amount of adsorbed fibrinogen.[33,34] However, the OMe-PRX-PMB surface showed a different tendency compared to those of the other materials surfaces. In particular, it is thought that the modulated conformational change of the adsorbed proteins, including fibrinogen on the dynamic OMe-PRX-PMB surface, can prevent platelet adhesion as discussed in Fig. 8 (b), in spite of the significant amounts of adsorbed proteins.

Fig. 10 (a) shows the resulting optical microscopic images of the polymer surfaces. Clearly, large numbers of fibroblasts were

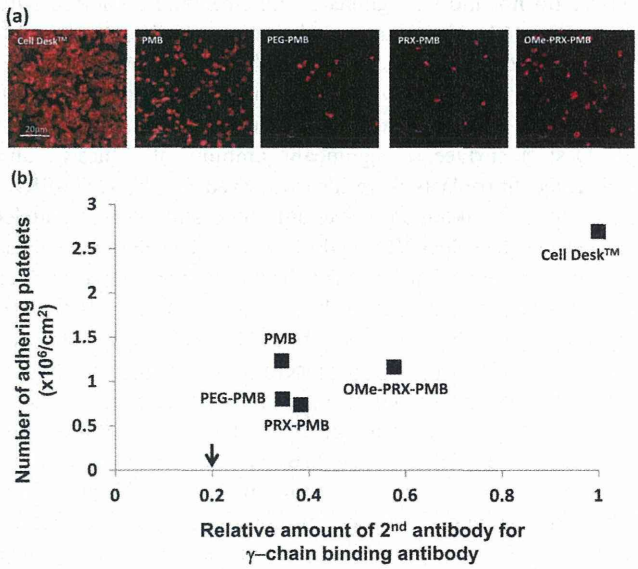

Fig. 9 (a) Fluorescent microscopic image of adhering platelets and (b) quantitative analysis of adhering platelets using LDH assay (n = 3). The plot also shows the relative amount of the secondary antibody for the C-terminus γ-chain binding antibody (normalized to the Cell Desk™). The arrow indicates the background level of ELISA. PRP contact was carried out for 3 h at 37 °C. Scale bar = 200 μm.